Iraqi Journal of Biotechnology, 2026, Vol. 25, No. 2, 56-69

Photosynthesized Selenium Nanoparticles using Aas (*Myrtus communis* L.) Leaves Extract

[1,2]Dhuha H. Al Jubouri, Esam J. Alkalifawi

[1,2]Department of Biology, College of Education for Pure Science (Ibn Al-Haitham), University of Baghdad, Baghdad, Iraq.

Abstract

Background: Selenium nanoparticles (SeNPs) have attracted considerable attention due to their unique physicochemical properties and broad biomedical applications. Green synthesis using plant extracts offers an eco-friendly and cost-effective approach for nanoparticle production. **Aim:** This study aimed to biosynthesize selenium nanoparticles using the leaf extract of Aas (Myrtus communis L.) and characterize the synthesized nanoparticles using various analytical techniques. **Methods:** Photosynthesized selenium nanoparticles (MC-SeNPs) were prepared using Myrtus communis leaf extract. The synthesized nanoparticles were characterized by ultraviolet-visible spectroscopy (UV-Vis), Fourier-transform infrared spectroscopy (FT-IR), X-ray diffraction (XRD), field emission scanning electron microscopy (FE-SEM), energy-dispersive X-ray spectroscopy (EDX), and atomic force microscopy (AFM). **Results:** The formation of MC-SeNPs was confirmed by the color change of the reaction mixture from colorless to reddish. UV-Vis analysis showed a characteristic absorption peak at 260 nm, indicating the surface plasmon resonance of SeNPs. FT-IR spectra confirmed the presence of functional groups involved in nanoparticle synthesis and stabilization. XRD analysis revealed diffraction peaks at 2θ values of 28.61°, 31.19°, 40.01°, 45.02°, 56.21°, 66.23°, 75.11°, and 84.74°, corresponding to the crystalline selenium phase. FE-SEM images demonstrated predominantly spherical nanoparticles aggregated into clusters, with particle sizes ranging from 21.86 to 31.94 nm. The crystallite size calculated using the Debye–Scherrer equation ranged between 21 and 31 nm. EDX analysis confirmed the presence of selenium along with oxygen, carbon, sodium, and copper. AFM analysis revealed homogeneous spherical nanoparticles with sizes ranging from 20 to 30 nm. **Conclusion:** The leaf extract of Myrtus communis can be successfully utilized for the green synthesis of selenium nanoparticles. The phytochemical constituents of the extract act as reducing and capping agents, producing stable, crystalline, and predominantly spherical selenium nanoparticles suitable for potential future applications.

Keywords: *Myrtus communis* L.; Photosynthesis; Selenium NPs; Charactrization.

Corresponding author: (E-mail: wrdta3965@gmail.com).

Introduction

The size and morphology of synthesized metallic nanoparticles can be controlled with chemical reducing agents (1, 2). However, the reducing agents and solvents used in the synthesis of nanoparticles are hazardous or toxic to the environment (3). Consequently, the Photosynthesis of nanoparticles is anticipated, even though there are several categories of Phyto reductants (based on isolation/extraction sources) existing in nature. Under these circumstances, Photosynthesis approaches can significantly assist with the preparation of metal nanoparticles (4,5). In recent times, the tendency to use natural materials such as microorganisms(6), marine organisms

(7), proteins (8), and plant extracts (PE) used in the green synthesis of metallic NPs has attained significant consideration in the scientific community (9).

Especially metal nanoparticle synthesis using plant extracts has been given more attention due to plants being easily available, inexpensive, environmentally friendly and also the ability to highly reduce the usage of toxic solvents or reducing agents (10). Medical plants and their extracts were used as traditional treatments for several diseases in various parts of the world for many thousands of years (10), particularly in rural areas of these countries; they were used as a primary source of medicine (9). In developing countries, 80% of the population uses natural products in routine healthcare practice (11).

Aas (*Myrtus communis* L.) (Family: Myrtaceae) plant is most widely used as a medicinal drug in unani medicine since the earliest historical times in Greece (12).

It is an herb with rich contents of flavonoids, alkaloids, tannins, terpenoids and saponins, the biologically active ingredients used in traditional and alternative medicine (13), which makes it attractive for the green synthesis of silver nanoparticles. It is known as Aas and its berries are recognized (14). Several investigations revealed that Aas (*Myrtus communis* L.) possesses therapeutic and pharmacological effects showing anticancer, antimicrobial, antidiabetic properties, as well as neuro and hepato proactive activity (15, 16, 17). Aas (*Myrtus communis* L.) Leaves, berries and essential oils are commonly used for several disorders like ulcers, gastritis, rheumatism, diarrhoea, haemorrhages (18), dysentery, vomiting, deep sinuses, leucorrhoea and in hair loss control (19). The leaves, berries and twigs are used in flavoring food and wines (19). In earlier times, ripe fruits were utilized as food integrators due to their rich constituents of vitamins (20).

Selenium is an essential element that humans and animals require, which boosts the activity of enzymes like glutathione peroxidase (GPx) and selenidase that protect the body from immune-related disorders (21). Generally, Selenium occurs naturally in crystalline, amorphous polymorphic structures and three forms: inorganic (selenite and selenate), organic (selenomethionine and selenocysteine), and nanoforms (22). An insufficient amount of Selenium in humans impacts the production of selenoprotein. It leads to a decrease in the activity of GPx, which ultimately results in a diminished capacity of tissue cells to withstand the damaging effects of oxidative stress. It also directly impacts the production and breakdown of nucleic acids, proteins, mucopolysaccharides, and enzymes, as well as cell division, reproduction, immunity, and the onset of metabolic diseases. In addition, a lack of Selenium can lead to several illnesses, including thyroid problems, diabetes, problems with reproduction, and obesity (23). Therefore, obtaining extra Selenium is very important. Recently, Selenium Nanoparticles were used as a new form of supplement, which attracted researchers because of their biocompatibility, bioavailability, and low toxicity (22, 23). These SeNPs are in a very steady colloidal state and have shown several biological activities, including the immune system, antibacterial, antimicrobial, antivirus, antifungal, antiparasitic, antidiabetic, antioxidation and anticancer activities. SeNPs have demonstrated promise as a material to

address several issues brought on by low redox activity, ROS generation, and biofilm formation. SeNPs are better for food safety than organic Se and inorganic Se compounds like selenite and selenate. They are used as antibacterial nanocoating in food packaging and functional foods because they are nontoxic, easily dispersed, and have a large surface area (15, 16, 17). Selenium can also be utilized in fertilizers to stimulate plant growth, raise crop productivity, and facilitate the cultivation of Se-enhanced crops. However, SeNPs are not stable and tend to stick together. This is why it is essential to find easy and effective ways to make SeNPs more stable and spread out (13). Furthermore, they have been engineered for nutritional supplementation and have been developed for medical purposes (9, 10).

The present study summarizes Photosynthesized Selenium Nanoparticles using Aas (*Myrtus communis* L.) Leaves Extract and its characterization.

Materials and Methods

Materials

The Aas (*Myrtus communis* L.) plant which widely exists in the southern zone of Baghdad, was procured from a local herbal market at Towatha, Baghdad, Iraq.

The plant identification was confirmed by by Taxonomist in the Department of Biology, College of Education for pure science Ibn-Alhatheam, University of Baghdad. Na_2SeO_3 (99.8%) and other solvents utilized in this study were procured from Sigma Aldrich, St. Louis, MO, USA.

Preparation of Plant Extract

Initially, the leaves of Aas (*Myrtus communis* L.) were cut into tiny parts. The resulting tiny parts (500 gms) were soaked in 2.5 L deionized water and refluxed at boiling temperature for 6 h. The resultant aqueous solution after reflux was separated and dried up at 50-60°C underneath reduced pressure in a rotary evaporator to give a light yellow colored extract (40 gms). Furthermore, the separated extract was kept refrigerated at 0-4°C for further use.

Synthesis and Characterization of Selenium Nanoparticles using Aas (*Myrtus communis* L.) leaves Extract

The synthesis of Selenium nanoparticles was carried out by combining 10 mL of Aas (*Myrtus communis* L.) leaves extract with 0.5 mM Sodium selenite pentahydrate (85 mg) in 90 mL deionized water in a 250 mL round bottomed flask.

The reaction mixture was stirred with a magnetic bar for ~2 h at 90°C under refluxed conditions with a cooling condenser. During the reaction process, the reaction mixture color changed slowly from light yellow to reddish.

Afterwards, no color transformation was noticed till the completion of the reaction after two hours. Then, the reaction mixture was subjected to a cool down period, and later, the reaction mixture was centrifuged at 8000 rpm at room temperature. Subsequently, the product attained from the centrifugation was washed several times (three to four times) with deionized water.

After that, the product was dried overnight at 80°C in an oven and finally a black powder was obtained.

Characterization of Selenium nanoparticles

1- UV-Vis Spectra analysis:

The UV-Vis spectrum analysis was achieved within the range of 200 to 800 nm at a resolution of 0.86 nm using a UV-visible spectrophotometer (Shimadzu UV-1800). In this analysis Se

nanoparticles were examined at different reaction conditions. (24)

2- Fourier Transform Infra-Red Spectroscopy (FT-IR)

The FTIR analysis was introduced to investigate the chemical bonding between the atoms of the prepared materials nanoparticle. This particular technique was performed using the Shimadzu-IR Affinity-I spectrophotometer. In this procedure, the samples under test are homogenized with KBr and then the FTIR spectrum was recorded within the range of 4000 to 400 cm-1. Before the recording procedure, potassium bromide (AR-grade) was dried and mixed with KBr (100mg) as well as selenite (1 mg). Note that the KBr pellet was obtained under a vacuum with the temperature of 100°C for a period of 48hrs. (24)

3- X-Ray Diffraction (XRD) analysis

Resulting solution of the developed nanoparticles of Selenium was centrifuged at 10,000 rpm for 30 min. The solid residues of SeNPs were washed twice with deionized distilled water and then dried at 80º C to obtain powder SeNPs used for X-ray powder diffraction measurements. The powder of nanoparticles was measured by XRD. XRD patterns were recorded on (Shimadzu XRD-6000/Japan) with copper radiation (Cu Kα, 1.5406 Å) at 40 kV and 30 Ma (25).

4- Field emission scanning electron microscopy (FE-SEM) analysis

The images were taken with a Field emission scanning electron microscope (FE-SEM) (Hitachi Ltd. /Japan) with a resolution of 500 nm (Hitachi s-3400N) and detectors containing a secondary electron; BSE semiconductors (quad-type) were used to study the size and shape nanoparticles, this approach is used to obtain detailed information about surface NPS. FE-SEM was used to characterize the average particle morphology and diameter of the nanoparticles. After using distilled water to sonicate the dried nanoparticles solution sample, a tiny drop of the sample was put on a microscope slide and left to dry. The samples were then coated with a thin layer of platinum to make them conductive.

5- Energy Dispersive X-ray (EDX)

X-ray energy diffraction spectroscopy was used to investigate and determine the elemental compositions of the synthesized nanoparticles. For this purpose, after preparing the samples, using an EDX detector on field emission scanning electron microscope, the spectra of the constituent elements of the samples were prepared.

Atomic Force Microscope (AFM)

This technique aimed to investigate the surface morphology of the prepared Se nanoparticles using Inc. SPM-AA300 (U.S.) with AFM communication mode. In particular, 5 drops of nanoparticles solution were dropped on a specific laboratory slide and kept for 30 min at 110° C in an oven. Continuously, the 3D morphology /topography of the sample under the test surface was screened via the interaction of the probe force on the sample surface. This procedure is attained through a raster scan of the tested material, taking into consideration the distance and the force between the tip and the sample, two parameters that should be considered carefully (26). The AFM was introduced to investigate the Se nanoparticles' surface features using a 2D and 3D imaging approach.

Results

The prepared SeNPs were characterized by various spectroscopic and microscopic methods to evaluate their elemental composition, exact morphology and also other physicochemical properties. The color change of the reaction mixture from uncolored to reddish confirms the synthesis of MC-SeNPs Figure (1).

Figure (1): The change in the color of Photosynthesized Selenium Nanoparticles using Aas (*Myrtus communis* L.) Leaves Extract, A, Sodium selenite solution. B, Aas (*Myrtus communis* L.) Leaf Extract. C. Photosynthesized Selenium Nanoparticles colloidal.

The UV-Visible spectroscopy analysis revealed the absorption maximum (λmax) at 260 nm was attributed to the surface plasmon resonance (SPR) of MC-SeNPs Figure(2).

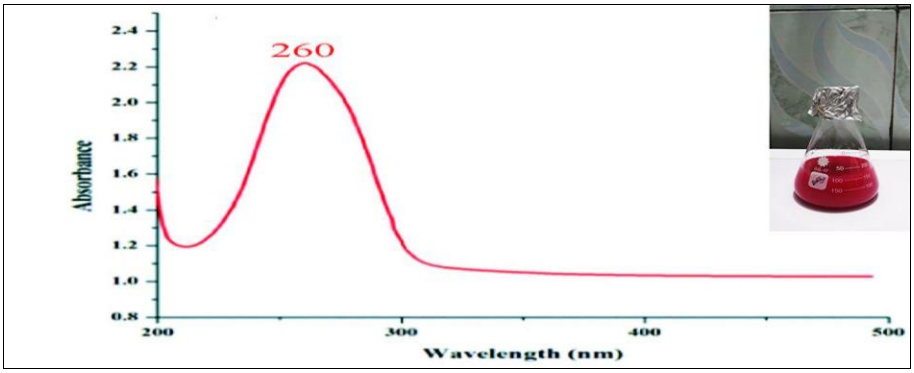

Figure (2): UV-Vis spectra of Photosynthesized Selenium Nanoparticles using Aas (*Myrtus communis* L.) Leaves Extract (MC-SeNPs).

The FT-IR analysis for the MC-SeNPs shows in figure 3 and table1. The intensive absorption peak at 3623 cm^{-1} was assigned to hydroxyl group (-OH) stretching of the aromatic ring and a sharp peak at 2923 cm^{-1} showing ether – methoxy-OCH_3 groups, while peak at 2852 and 1740 cm^{-1} represent the stretching of C=O aldehydes group, 1602 cm^{-1} (amide and CH vibrations of CH_2 group), 1457 cm^{-1} (CH group), 1261 cm^{-1} (Secondary -OH bending), 1114 and 805 cm^{-1} (C=O stretching vibrations, aromatic carbon vibrations and CH in plane benching).

Finally, the selenium compounds responsible for a broad frequency a range about of 675.04-420.45 cm^{-1}.

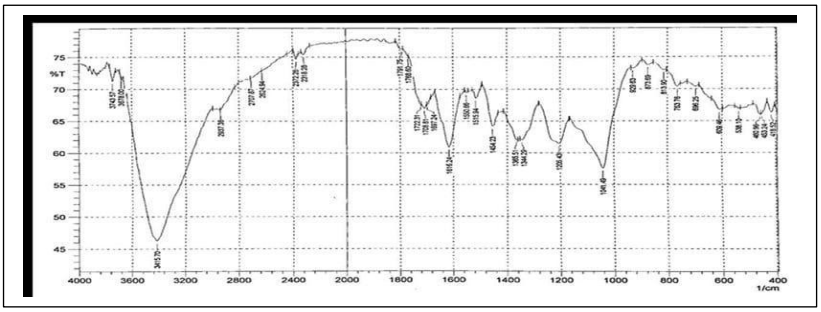

Figure (3): FT-IR spectra of (*Myrtus communis* L.) leaves extract

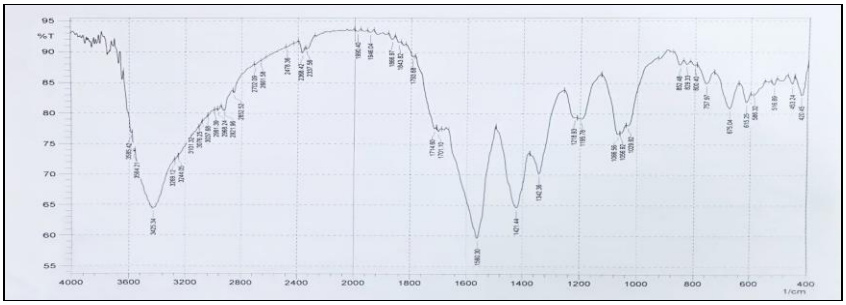

Figure (4): FT-IR spectra of Photosynthesized Selenium Nanoparticles using Aas (*Myrtus communis* L.) leaves extract (MC-SeNPs).

Table (1): Active groups present in the leaves extract of Aas (*Myrtus communis* L.) which act as reducing and capping agent for selenium nanoparticles.

LR. Wave number standard group of M. (*M communis*) Extract	Frequency of Absorption (cm^{-1})	Bonds	Compound class of Functional Groups
2700 .30	3425.34	O–H stretch	Alcohol
2140.34	1560.30	C=C stretch	Alkene
1450.40	1421.44	C–H bend	Alkene
1420-1330	1342.36	O–H bend	Alcohol
1250-1020	1218.93-1195.78	C–N stretch	Amine
1085-1050	1066.56-1029.92	C–O stretch	Alcohol
1070-1030	675.04-420.45	Metal Oxide	SeO

X-ray diffraction is generally applied to a certain chemical arrangement and crystal design of an objective and it can be used for exposing the presence of SeNPs. The specified crests are coordinated with the diffraction information of Se nanoparticles, the diffraction peaks of SeNPs were at 2θ = 28.61, 31.19, 40.01, 45.02, 56.21, 66.23, 75.11 and 84.74 were for the (100), (101), (110), (102), (111), (201), (112) and (202) reflections of the pure phase of selenium crystals. In the meanwhile, the crystalline particles were calculated using the well-known Debye-Scherrer equation:

$$\mathbf{D = (K\lambda/\beta\cos\theta)\ Å}$$

Herein, the crystallite size is represented by the symbol (D), while K denotes the shape factor which is a constant (0.9) and λ is the x-ray wavelength (1.5406 Å).

The Bragg angle and corrected line broadening of the nanoparticles are

represented by the symbols θ and β, respectively (26).

The average crystallite size according to Debye-Scherrer equation calculated was found to be 21-31 nm.

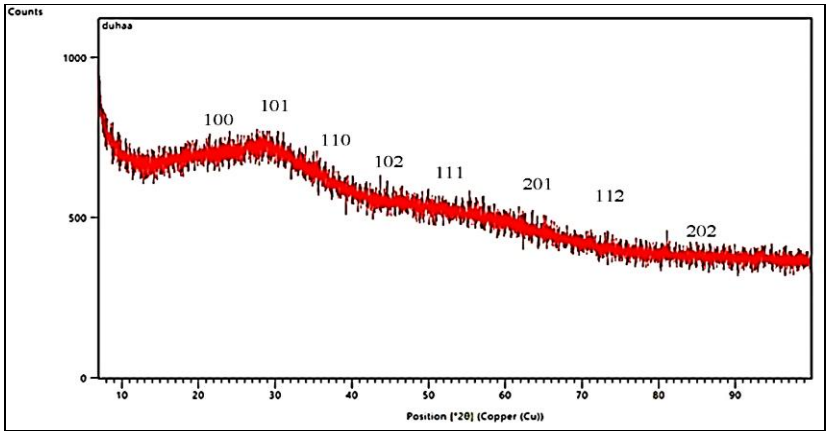

Figure (5): X-ray diffraction spectra of Photosynthesized Selenium Nanoparticles using Aas (*Myrtus communis* L.) Leaves Extract (MC-SeNPs).

Field Emission Scanning Electron Microscopy

Figure (4) shows a typical surface of prepared (MC-SeNPs) from sodium selenite using Aas (*Myrtus communis* L.) Leaves Extract reduction, the FESEM picture revealed a spherical in shape and aggregated into clusters. The size of these particles ranges from (21.86 - 31.94) nm.

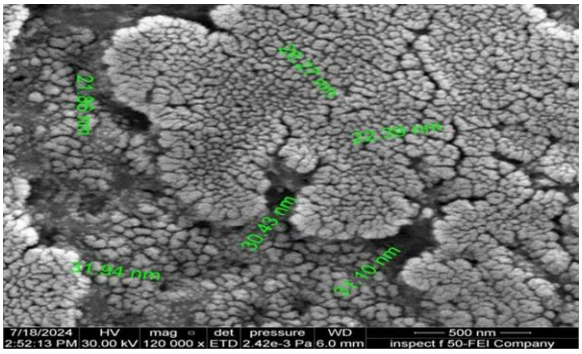

Figure (6): Field emission scanning electron microscopy image of Photosynthesized Selenium nanoparticles using Aas (*Myrtus communis* L.) Leaves Extract (MC-SeNPs).

EDX elemental analysis of Photosynthesized Selenium nanoparticles using Aas (*Myrtus communis* L.) Leaves extract exhibits the selenium signal along with carbon, oxygen, sodium and copper; among these, the copper signal arises from the copper-coated grid, sodium may be from Aas leaves extract. The EDX spectrum shown in Figure (5), confirms the presence of an elemental form of selenium.

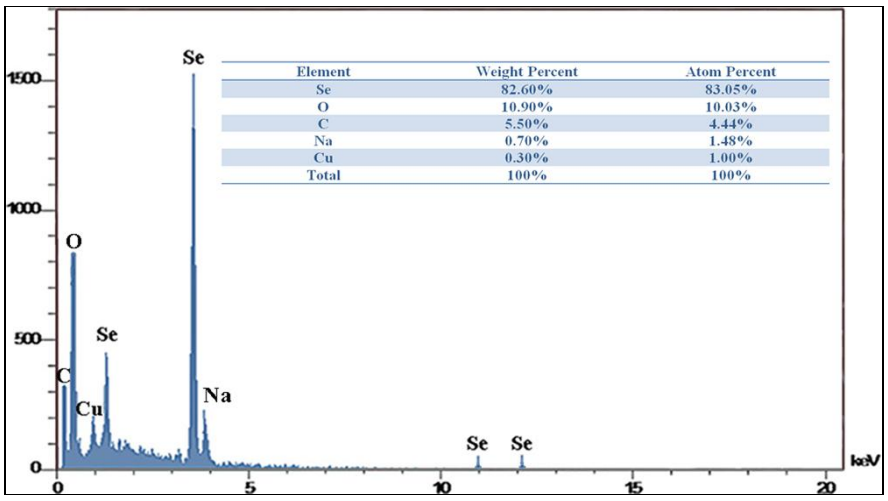

Element	Weight Percent	Atom Percent
Se	82.60%	83.05%
O	10.90%	10.03%
C	5.50%	4.44%
Na	0.70%	1.48%
Cu	0.30%	1.00%
Total	100%	100%

Figure (7): EDX elemental analysis of Photosynthesized Selenium nanoparticles using Aas (*Myrtus communis* L.) Leaves extract (MC-SeNPs).

Through atomic force microscopic analysis, the three-dimensional profile of the Photosynthesized Selenium nanoparticles using Aas (*Myrtus communis* L.) Leaves Extract revealed the shape, porosity, surface topography, and height of the MC-SeNPs. Figure 6 shows the atomic force photomicrograph depicting the spherical-shaped nanoparticles distributed in a polydisperse manner, which also correlates with FE-SEM results. It is very clear from the 3D profile of MC-SeNPs that the surface of the nanoparticle was smooth, and the average height of the nanoparticles was measured at 30 nm.

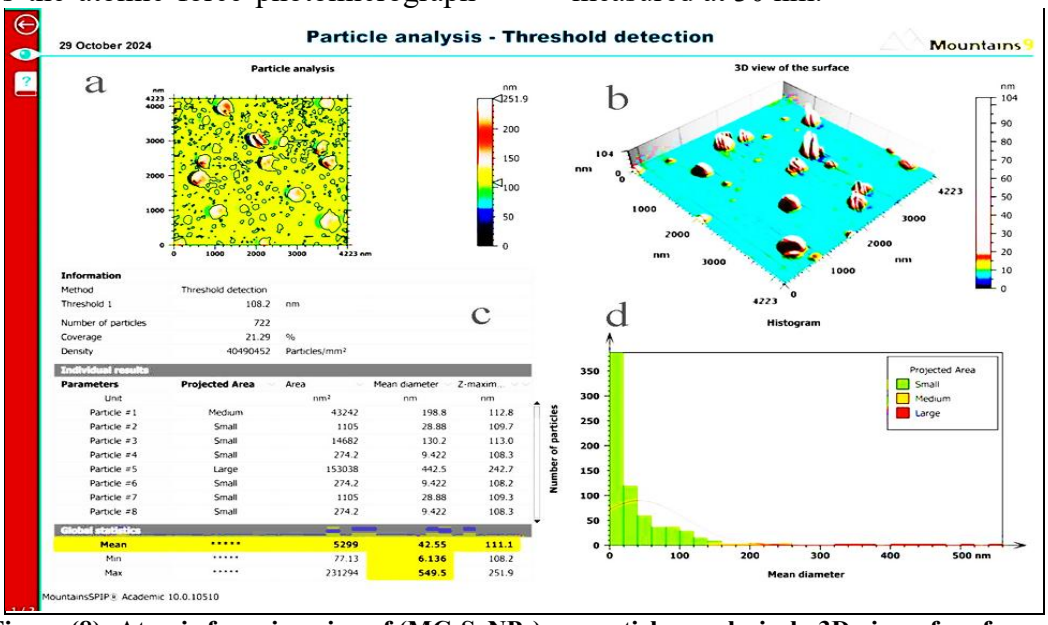

Figure (8): Atomic force imaging of (MC-SeNPs). a, particles analysis, b, 3D view of surface, c, minimum and maximum of diameter and d, mean diameter.

The 2D image of the Photosynthesized Selenium nanoparticles using Aas (*Myrtus communis* L.) Leaves Extract shows smaller individual particles

of about 21.86 nm in size, along with larger agglomerates of sizes up to ~150 nm while the 3D image indicates the presence of individual spherical particles, with a maximum height of 32.55 nm in the z-direction.

Discussion

The present study was conducted considering the importance of selenium nano-particles, it's have remarkable absorption, low toxicity, and exhibit antioxidant and antibacterial effects. Selenium, an essential nutritional vitamin, is a relatively new member of Nano pharmaceutical medicine in healthcare (27).

Selenium nanoparticles were prepared using Aas (*Myrtus communis* L.) Leaves Extract (MC-SeNPs). The advantage of this method is that using plant extracts as reducing and capping agents is a fast and easy approach to make environmentally friendly metal nanoparticles. This synthesis is environmentally and bio-reduced, involves only one step, is affordable, requires only a small number of solvents and requires less reaction time. There are several physical, chemical and biophysical processes to makeing selenium nanoparticles. However, some of the methods are expensive, use hazardous chemicals, and involve laborious, time-consuming and unsustainable practices. Hence, Photosynthesis methods are preferred over those based on chemical and physical procedures (28, 29, 30, 31).

The prepared SeNPs were characterized by various spectroscopic and microscopic methods to evaluate their elemental composition, exact morphology and also other physicochemical properties. The color change of the reaction mixture from uncolored to reddish confirms the synthesis of MC-SeNPs. These findings are consistent with several studies (32, 33, 34) that reported a change in the color of the selenite solution from colorless to purple-red after mixing it with the plant extract, indicating the completion of the reaction and the formation of selenium nanoparticles. UV-Vis absorption spectra were recorded for the indication of the Se nanoparticles formation. The absorption spectra showing the corresponding absorption maxima at 260 nm, confirmed the formation of MC-SeNPs and indicated surface plasma resonance of the MC-SeNPs. Absorption spectra of MC-SeNPs showing the stability of MC-SeNPs, demonstrate that the Aas (*Myrtus communis* L.) leaves extract not only acts as a reducing and capping agent, but also that the phytoconstituents of MC functionalized the surface of MC-SeNPs. These results are in agreement with several studies (35, 36, 37) that reported that the absorption peak of selenium nanoparticles using the UV-visible analysis assay is located in the absorption range of 200-400 nm. FT-IR analysis of MC-SeNPs was used to characterize the presence of functional groups responsible for the synthesis and stability of selenium nanoparticles. The intensive absorption peak at 3623 cm^{-1} was assigned to hydroxyl group (-OH) stretching of the aromatic ring and a sharp peak at 2923 cm^{-1} showing ether –methoxy-OCH_3 groups, while the peak at 2852 and 1740 cm^{-1} represent the stretching of C=O aldehydes group, 1602 cm^{-1} (amide and CH vibrations of CH_2 group), 1457 cm^{-1} (CH group), 1261 cm^{-1} (Secondary -OH bending), 1114 and 805 cm^{-1} (C=O stretching vibrations, aromatic carbon vibrations and CH in plane benching).

Finally, the selenium compounds are responsible for a broad frequency range about of 675.04-420.45 cm^{-1}. This result indicates the presence of various functional groups as biomolecules which may be responsible for both reduction and stabilization of the MC-SeNPs. Previous reports have also suggested the role of phytochemicals as a stabilizing agent for the synthesis of metal NPs (38, 39,40). X-ray diffraction is generally applied to a certain chemical arrangement and crystal design of an objective and it can be used for exposing the presence of SeNPs. The specified crests are coordinated with the diffraction information of Se nanoparticles, the diffraction peaks of SeNPs were at 2θ = 28.61, 31.19, 40.01, 45.02, 56.21, 66.23, 75.11 and 84.74 for the (100), (101), (110), (102), (111), (201), (112) and (202) reflections of the pure phase of selenium crystals. The average crystallite size calculated by the Debye-Scherrer equation was found to be 21-31 nm. These findings are in agreement with several studies (26, 40, 41) that reported the diffraction peaks of SeNPs start at 100, 101, 110,102, 111, 201, 112, and end at 202. The size average and form of nanoparticles in the test sample may be determined using FESEM imaging, which is an analytical method. The FESEM image revealed a spherical shape and aggregated into clusters. The size of these particles ranges from (21.86, 22.39, 26.27, 30.43, 31.10 and 31.94) nm. These results are in agreement with several studies (42, 43) that reported that in most biosynthesis methods, the FESEM picture revealed a spherical shape and the size of these particles ranges from 20-40 nm. In the EDX spectrum of Photosynthesized SeNPs using Aas (*Myrtus communis* L.) Leaves extract, in addition to oxygen and selenium, carbon, oxygen, sodium and copper elements were also observed, the copper signal arises from the copper-coated grid, and sodium may be from Aas leaves extract. The EDX spectrum of MC-SeNPs indicates the presence of some impurities due to the biological synthesis of nanoparticles. These findings are in agreement with several studies (44, 45) that reported the EDX analysis helps to determine the purity and elemental composition of the sample. AFM is very important technique, which is used to get the information about particle size, shape, surface topography, and so forth. Therefore,the morphology and structure of the Photosynthesized Selenium nanoparticles using Aas (*Myrtus communis* L.) Leaves Extract were also determined by this technique. The 2D image of the Photosynthesized Selenium nanoparticles using Aas (*Myrtus communis* L.) Leaves Extract shows smaller individual particles of about 21.86 nm size, along with larger agglomerates of sizes up to ∼150 nm while the 3D image indicates the presence of individual spherical particles, with maximum height of 32.55 nm in the z-direction. These findings are in agreement with several studies (46, 47, 48) that reported that in the almost photosynthesis methods of SeNPs, the AFM images show smaller individual particles of about 20-40 nm.

Conclusions

We conclude from the present study the possibility of using the leaves extract of the Aas (*Myrtus communis* L.) to prepare selenium nanoparticles because the leaves of this plant are known for their rich content of flavonoids, alkaloids, tannins, terpenoids, and saponins, which appear to have the ability to reduce

selenite salts and convert them into selenium nanoparticles and also act as a capping agent.

Acknowledgments

Thanks and appreciation to Dr. Labib, Ministry of Science and Technology, Dr. Laith, Department of Biotechnology/University of Baghdad, and Dr. Arrej Alani, Department of Biology, College of Education for pure science Ibn-Alhatheam, University of Baghdad. For their assistance in diagnosing the Aas plant and conducting tests on the properties of the nanomaterial.

References

1. Szczyglewska, P., and A. Feliczak-Guzik, and I. Nowak, (2023). Nanotechnology–General Aspects: A Chemical Reduction Approach to the Synthesis of Nanoparticles. Molecules, 28(4932): 1-38.
2. Al-Salhie, H. H., and Al-Kalifawi, E. J. (2020). Antimicrobial and antivirulence activity of magnesium oxide nanoparticles synthesized using *klebsiella pneumonia* culture filtrate. Biochemical and Cellular Archives, 20(2): 3325-32.
3. Biswas, A. (2024). Synthesis and Characterization of Colloidal Silver nanoparticles of about 16 nm Diameter by a Chemical Reduction Method. Orient. Journal of Chemistery, 40(4): 1035-39.
4. Hameed, H. Q., Hasan, A. A., and Abdullah, R. M. (2019). Effect of Olea europea L Extraction and TiO 2 Nanoparticles against *Pseudomonas aeruginosa*. Indian Journal of Public Health Research and Development, 10(6).
5. Li, P., Y. Xia, K. Song, and D. Liu, (2024). The Impact of Nanomaterials on Photosynthesis and Antioxidant Mechanisms in Gramineae Plants: Research Progress and Future Prospects. Plants, 13(984): 1-22
6. Kato, Y. and M. Suzuk, (2020). Synthesis of Metal Nanoparticles by Microorganisms. Crystals, 10(589): 1-22.
7. dos Santosa, V. C. T., L. F. Cusiolib, L. Nishib, C. A. Ottonia, and R. Bergamasco, (2024). Metallic nanoparticles synthesized by marine microorganisms and its application against pathogenic microorganisms: Challenges and opportunities in marine nanotechnology. Desalination and Water Treatment, (317) 100283: 1-8.
8. Muhahid Abdullah Al-Shuwaikh, A., Mujahid Abdullah Al-Shwaikh, R., and Hassan, J. S. (2019). Effect of *Trigonella foenum* Extract and ZiO_2 Nanoparticles on Some Pathogenic Fungi and Bacteria. La Prensa Médica Argentina: 302-308.
9. Goswami, N., R. Saha, and S. K. Pal, (2011). Protein-assisted synthesis route of metal nanoparticles: Exploration of key chemistry of the biomolecule Journal of Nanoparticle Research, 13(10): 5485-95.
10. Pyrzynska, K. (2024). Plant Extracts for Production of Functionalized Selenium Nanoparticles. Materials, 17(3748): 1-19.
11. Chaughule, R. S. and R. S. Barve, (2024). Role of herbal medicines in the treatment of infectious diseases. Vegetos, 37:41-51.
12. Ferreira, E. da C., M. da G. V. Anselmo, N. M. Guerra, C. M. de Lucena, C. do M. P. Felix, R. W. Bussmann, N. Y Paniagua-Zambrana, and R. F. P. de Lucena, (2021). Local Knowledge and Use of Medicinal Plants in a Rural Community in the Agreste of Para´ıba, Northeast Brazil. Evidence-Based Complementary and Alternative Medicine, Article ID 9944357: 1-16.
13. Asase, A. (2023). Ghana's herbal medicine industry: prospects, challenges and ways forward from a developing country perspective. Front. Pharmacol; 14:1267398.
14. Sisay, M. and T. Gashaw, (2017). Ethnobotanical, Ethnopharmacological, and Phytochemical Studies of *Myrtus communis* Linn: A Popular Herb in Unani System of Medicine. Journal of Evidence-Based Complementary and Alternative Medicine, 22(4): 1035-43.
15. Al-Maharik, N., N. Jaradat, N. Al-Hajj and S. Jaber, (2023). *Myrtus communis* L.: essential oil chemical composition, total phenols and flavonoids contents, antimicrobial, antioxidant, anticancer, and α-amylase inhibitory activity. Chemical and Biological Technologies Agriculture, 10(41): 1-13.
16. Abuderman, A. A., R. Syed, A. A. Alyousef, M. S. Alqahtani, M. S. Ola and A. Malik,

(2019). Green Synthesized Silver Nanoparticles of *Myrtus communis* L (AgMC) Extract Inhibits Cancer Hallmarks via Targeting Aldose Reductase (AR) and Associated Signaling Network. Processe, *7*(11) 1-13.

17. Muhsen, T. A., Hawar, S. N., Mahdi, T. S., and Khaleel, R. (2020). Effect of Eucalyptus and Myrtus extracts identification by gas chromatography-mass spectrometry on some species of Candida as amodel of medical plants. Ann. Trop. Med. and Public Health, 23(S10), 1-11.
18. Mir, M. A., L. A. Memish, S. E. Elbehairi, N. Bashir, F. S. Masoud, A. A. Shati, M. Y. Alfaifi, A. M. Alamri, S. A. Alkahtani and I. Ahmad, (2024). Antimycobacterial and anticancer properties of *Myrtus communis* leaf extract. Pharmaceuticals (Basel), 17(7): 1-19.
19. Parlak, T. M., B. Traş, K. Üney, and B. S. Alan, (2024). Antidiabetic Effect of Hydro-alcoholic Extract of *Myrtus communis* L. Fruit in a Type 2 Diabetes Mouse Model. Acta Vet Eurasia, 50(3): 210-7.
20. Barhouchi, B., R. Menacer, S. Bouchkioua, A. Mansour, and N. Belattar, (2023). Compounds from myrtle flowers as antibacterial agents and SARS-CoV-2 inhibitors: *In-vitro* and molecular docking studies. Arabian Journal of Chemistry, 16(8): 1-12.
21. Mohammad, M. A., and Hasan, M. A. (2024). Effect of organic selenium and vitamin e on some blood and biochemical parameters in common carp *Cyprinus carpio* L. Iraqi Journal of Agricultural Sciences, 55(4), 1360-66.
22. Mir, M. A. (2024). *Myrtus communis* leaves: source of bio-actives, traditional use, their biological properties, and prospects. Boletín Latinoamericano y del Caribe de Plantas Medicinales y Aromáticas, 23(4): 487-515.
23. Giampieri, F., D. Cianciosi, and T. Y. Forbes-Hernández, (2020). Myrtle (*Myrtus communis* L.) berries, seeds, leaves, and essential oils: New undiscovered sources of natural compounds with promising health benefits. Food Frontiers, 1: 276-95.
24. Wali, A. T. and Alqayim, M.A.J. (2019). Biosynthesis, characterization and bioactivity of selenium nanoparticles synthesized by propolis. The Iraqi Journal of Veterinary Medicine, 43(1): 197-209.
25. El-Deeb, B., Al-Talhi, A., Mostafa, N., and Abou-assy, R. (2018). Biological synthesis and structural characterization of selenium nanoparticles and assessment of their antimicrobial properties. Am. Sci. Res. J. Eng. Technol. Sci, 45(1), 135-70
26. Lebaka, V. R., Y. J. Wee, W. Ye, and M. Korivi, (2021). Nutritional Composition and Bioactive Compounds in Three Different Parts of Mango Fruit. Int. J. Environ. Res. Public Health, 18: 741.
27. Zhang, F., X. Li, and Y. Wei, (2023). Selenium and Selenoproteins in Health. Biomolecules, 13(799): 1-25.
28. Mojadadi, A., A. Au, W. Salah, P. Witting, and G. Ahmad, (2021). Role for Selenium in Metabolic Homeostasis and Human Reproduction. Nutrients, 13, 3256.
29. Sampath, S., V. Sunderam, M. Manjusha, Z. Dlamini, and A. V. Lawrance, (2024). Selenium Nanoparticles: A Comprehensive Examination of Synthesis Techniques and Their Diverse Applications in Medical Research and Toxicology Studies. Molecules, 29(801):1-24.
30. Tabibi, M., S. Aghaei, M. A. Amoozegar, R. Nazari and M. R. Zolfaghari, (2023). Characterization of green synthesized selenium nanoparticles (SeNPs) in two different indigenous halophilic bacteria. BMC Chemistry, 17: 115.
31. Bellotti, R., G. B. Picotto, and L. Ribotta, (2022). AFM Measurements and Tip Characterization of Nanoparticles with Different Shapes. Nanomanufacturing and Metrology, 5:127-38.
32. Nasiri, S., M. Rabiei, A. Palevicius, G. Janusas, A. Vilkauskas, V. Nutalapati, A. Monshi, (2023). Modified Scherrer equation to calculate crystal size by XRD with high accuracy, examples Fe_2O_3, TiO_2 and V_2O_5. Nano Trends, 3: 100015.
33. Liu, S., W. Wei, J. Wang and T. Chen. (2023). Theranostic applications of selenium nanomedicine against lung cancer. Journal of Nanobiotechnology, 21(96): 1-35.
34. Nyabadza, A.,´E. McCarthy, M. Makhesana, S. Heidarinassab, A. Plouze, M. Vazquez, and D. Brabazon, (2023). A review of physical, chemical and biological synthesis methods of bimetallic nanoparticles and applications in sensing, water treatment,

biomedicine, catalysis and hydrogen storage. Advances in Colloid and Interface Science, 321: 1-44.

35. Al-Khafaji, A. R. and A. H. Al-Azawi, (2022). Green Method Synthesis of Silver Nanoparticles Using Leaves Extracts of *Rosmarinus officinalis*. Iraqi Journal of Biotechnology, 21(2): 251-67.
36. Ali, Z. A. S. and A. M. Y. AL-Araji, (2024). Effectivity of Copper Nanoparticle Synthesis by *Fusarium oxysporum* Culture Filtrate as an Antimicrobial Agent against *Streptococcus thoraltensis* and *Proteus mirabilis*. Iraqi Journal of Biotechnology, 23(3): 194-208.
37. AL-Kalifawi, E. J., Y. J. Kadem, and I. I. Hazzaa, (2015). Green synthesis of Magnetite Iron Oxide Nanoparticles using Al-Rawag tree (*Moringa oleifera* Lamarck) leaves Extract and Used in Tigris River Water Treatment. Iraqi Journal of Biotechnology, 14(2): 29-43.
38. Puri, A., P. Mohite, S. Patil, V. R. Chidrawar, Y. V. Ushir, R. Dodiya and S. Singh, (2023). Facile green synthesis and characterization of *Terminalia arjuna* bark phenolic–selenium nanogel: a biocompatible and green nano biomaterial for multifaceted biological applications. Frontiers in Chemistry, 11: 1273360.
39. Al-Abdeli, I. H. and E. J. Al-kalifawi, (2023). Gold Nanoparticle Biosynthesis-Mediated *Acinetobacter Ƅaumannii* as a Cytotoxic and Apoptosis Inducer in Prostate Cancer Cell Lines. The Egyptian Journal of Hospital Medicine, 91: 3885-95.
40. Ubaid, H. N. and E. J. Alkalifawi, (2022). Biofabrication of silver nanoparticles using *E. camaldulensis* leaf extract and its antibacterial activity against multidrug resistance *Escherichia coli* and *Klebsiella pneumoniae* isolated from urinary tract infections. Biochemical and Cellular Archives, 22(1): 381-90.
41. Shahabadia, N., S. Zendehcheshma, and F. Khademic, (2021). Selenium nanoparticles: Synthesis, *in-vitro* cytotoxicity, antioxidant activity and interaction studies with ct-DNA and HSA, HHb and Cyt c serum proteins. Biotechnology Reports, 30: 1-21.
42. Hernández-Díaz, J. A.; J. J. O. Garza-García; J. M. León-Morales; A. Zamudio-Ojeda; J. Arratia-Quijada; G. Velázquez-Juárez; J. C. López-Velázquez; and S. García-Morales, (2021). Antibacterial Activity of Biosynthesized Selenium Nanoparticles Using Extracts of Calendula officinalis against Potentially Clinical Bacterial Strains. Molecules, 26: 5929.
43. Behera, A., devi M. S. Yamuna, I. Ryntathiang, and M. K. D. Jothinathan, (2024). Green Synthesis of Selenium Nanoparticles using *Cinnamomum verum* Extract and their Antibacterial, Antioxidant, and Brine Shrimp Toxicity Effects. Texila International Journal of Public Health: 1-13.
44. Al-Kalifawi, E. J., Y. J. Al-Azzawi1 and M. A. Feaza, (2021). Antibacterial, antivirulence and antifungal activity of silver nanoparticles synthesized using alkhal mother shae. Journal of Physics: Conference Series, 1879: 022054.
45. Al-Kalifawi, E. J. (2018). Silver Nanoparticles Synthesis by Hamza's Khubdat (A.S.) (Kombucha) Tea and used in Burn Wounds Treatment. Journal of Global Pharma Technology, 10(1): 489-500.
46. Souza, L. M. dos S., M. Dibo, J. J. P. Sarmiento, A. B. Seabra, L. P. Medeiros, I. M. Lourenço, R. K. T. Kobayashi, and G. Nakazato, (2022). Biosynthesis of selenium nanoparticles using combinations of plant extracts and their antibacterial activity. Current Research in Green and Sustainable Chemistry 5: 1-10.
47. Gharieb, M. M., A. M. Soliman, and M. S. Omara, (2023). Biosynthesis of selenium nanoparticles by potential endophytic fungi *Penicillium citrinum* and *Rhizopus arrhizus*: characterization and maximization. Biomass Conversion and Biorefinery: 1-10.
48. Lashani, L., H. Moghimi, R. J. Turner, and M. A. Amoozegar, (2024). Characterization and biological activity of selenium nanoparticles biosynthesized by *Yarrowia lipolytica*. Microbial Biotechnology, 17: e70013.
49. Mohammed T. J. and M. K. Abboud Al-Shibly, (2023). Therapeutic Effect of Biosynthesis of Selenium Nanoparticles on Enhancing Apoptosis Induction and Cell Lines Arrest in MCF-7 Breast Cancer Cell Lines. Nanostruct, 13(3): 796-805.
50. Jha, N. P. Esakkiraj, A. Annamalai, A. K. Lakra, S. Naik, and V. Aru, (2022). Synthesis, optimization, and physicochemical characterization of selenium nanoparticles from polysaccharide

of mangrove *Rhizophora mucronata* with potential bioactivities. Journal of Trace Elements and Minerals, 2: 100019.

51. Shahbaz, M., A. Akram, A. Mehak, E. U. Haq, N. Fatima, G. Wareen, B. N. Fitriatin, R. Z. Sayyed, N. Ilyas, and M. K. Sabullah, (2023). Evaluation of Selenium Nanoparticles in Inducing Disease Resistance against Spot Blotch Disease and Promoting Growth in Wheat under Biotic Stress. Plants, 12(761): 1-22.
52. Ramachandran, T., D. Manoharan, S. Natesan, S. K. Rajaram, P. Karuppiah, M. R. Shaik, M. Khan, and B. Shaik, (2023). Synthesis and Structural Characterization of Selenium Nanoparticles–Bacillus sp. MKUST-01 Exopolysaccharide (SeNPs–EPS) Conjugate for Biomedical Applications. Biomedicines, 11: 2520.
53. Abdul-Hamead, A. A. (2019). Fabrication and AFM characterization of selenium recycled nano particles by pulse laser evaporation and thermal evaporation. Materials Research Express, 6(12): 1-14.
54. Chetehouna, S., S. Derouiche, and Y. Reggami, (2024). Green Chemistry Approaches towards the Synthesis of Selenium Nanoparticles (SeNPs) as a Metal Nano-Therapy: Possible Mechanisms of Anticancer Action. Frontiers in Biomedical Technologies, 11(3): 509-29.